Time-dependent photoluminescence fatigue-recovery phenomena in germanium sulfide glasses

Takayuki Nakanishi[1], Yoichi Tomii, Kan Hachiya*

Department of Fundamental Energy Science, Graduate School of Energy Science,

Kyoto University, Sakyo-ku, Kyoto 606-8501, Japan

Abstract

Photoluminescence (PL) fatigue-recovery phenomena in germanium sulfide were investigated, and the temperature dependence of the time-dependent PL intensity for several compositions ($Ge_{33.3}S_{66.7}$, $Ge_{20}S_{80}$ and $Ge_{10}S_{90}$) was analyzed. Side-bands were observed and two bands out of them for argon-ion laser excitation, one at 2.25 eV for all compositions and the other extended from 2.15 to 2.45 for $Ge_{10}S_{90}$ especially at the lower temperatures, were used to fully describe the time-dependence.

The functional form which is similar to those in the previous report [T. Nakanishi et al., J. Non-Cryst. Solids 354 (2008) 1627] was used and it is extended to account for the effect of side-band at below 30 K for $Ge_{20}S_{80}$ and monotonous decrease of background for $Ge_{10}S_{90}$.

Keywords: chalcogenide glass, photoluminescence, photo-induced phenomena

1. Introduction

Chalcogenide glasses are one of the most prospective materials in amorphous semiconductors, and have attracted a number of researches. For example, phase-change

* Corresponding author. Tel: +81 774 38 4424; fax: +81 774 38 4462.
E-mail address: hachiya@energy.kyoto-u.ac.jp (K. Hachiya).
[1] Present address: Division of Materials Chemistry, Graduate School of Engineering, Hokkaido University, Sapporo, Hokkaido 060-8628, Japan.

optical disks using reversible switching between crystalline and non-crystalline states by light have been developed for chalcogenide thin films, Ge-Sb-Te or Ag-In-Sb-Te [1]. The chalcogenide compounds include chalcogen (group VI) elements such as sulfur, selenium and tellurium, which have high structural flexibility due to their twofold coordination. As a result of the structural flexibility, thin-film chalcogenides and chalcogenide glasses exhibit a variety of photo-induced phenomena in their optical and thermal properties such as photo-bleaching [2, 3], photoconductivity [4, 5], photo-expansion [6], etc. In particular, it is well known that the intensity of photoluminescence (PL) decreases through prolonged irradiation of bandgap or sub-bandgap light. This phenomenon is called PL fatigue [7]. To understand the origin of the PL fatigue, various reports [8-11] have been published. It is investigated that the phenomenon is strongly related to a photo-induced change of localized electronic states of defects, which is also the case with many other photo-induced phenomena. There are some models [12-19] for such defects. Nevertheless, these models need evidence.

Technological appliations of amorphous chalcogenides are expected toward those roughly categorized in two fields, utilizing two characteristic physical properties of these glasses described above: high-density optical storage making use of flexibility of chalcogens especially at photo-excited states; and glass materials for integrated optics making use of their high transparency at near-infrared region [20]. The above studies on PL give insight into bandgap states which possibly cause degradation of light transmission, and into meta-stability under photo-irradiation which is fundamental process of optical recording with photo-induced phenomena through transient PL measurements.

The purpose of the present study is to clarify the fundamental process of the photo-structural properties of Ge-S chalcogenide glass. Several reports can be found for PL from Ge-S glass [21-30]. Nevertheless, these properties have not been investigated compared with other chalcogenides. For this purpose, the relation between the origin of

photoinduced phenomena and the defect-related process including its temperature dependence should be elucidated for the Ge-S glass.

Seki et al. [28-30] investigated the electronic structures of $Ge_{1-x}S_x$ ($0.60 \leq x \leq 0.90$) chalcogenide glass, and provided a schematic for the electronic structures near bandgap for Ge-S glass and density of states (DOS) of Ge-S glass through both experiments and calculations [31, 32]. It is demonstrated in the series of studies that the charged and neutral center acts as radiative and non-radiative recombination centers, respectively [29].

In our previous study [33], temperature dependence of the photo-induced PL fatigue-recovery phenomena in GeS_2 glass was investigated. The mechanism of PL fatigue can be explained by photo-induced creation of meta-stable neutral defects D^0, which are non-radiative recombination centers. The recovery process, which is observed for the first time and proved to be a reverse process of the PL fatigue by Seki and Hachiya [29], depends apparently on temperature and restores the charged defects, surmounting an activation energy, ΔE, at the cost of heat energy.

In this paper, we focus not only on the fatigue-recovery mechanism of the main photoluminescence band, but also on those of the sub-bands for several Ge-S glasses. It is well known that the number density of defects, both of charged defects, D^-, D^+ and neutral defect D^0, change with their compositions [28, 34]. In particular, the content of sulfur affects the rate of photo-induced reaction. The relation between the phenomena and composition, or temperature, should provide a clue to understand the photoluminescence mechanism.

2. Experimental

2.1 Preparation of samples

The sample preparation process has already been described in a previous report [33]. Bulk $Ge_{20}S_{80}$ and $Ge_{10}S_{90}$ samples, other than $Ge_{33.3}S_{66.7}$ of Ge-S glasses were prepared

by the melt-quenching technique. The high purity raw materials were weighed and well mixed. The mixed powders were sealed in an evacuated fused silica ampoule ($\leq 5 \times 10^{-6}$ Torr). They were kept at 1173 K for 40 h in a furnace after 10 h of temperature elevation, quenched in ice water. Additionally, they were annealed at temperatures 50 K lower than their T_g [35], which is 331 K for $Ge_{20}S_{80}$ and 290 K for $Ge_{10}S_{90}$, in order to get rid of internal distortions and cracks. The non-crystalline nature of the samples was confirmed by an X-ray diffraction and the compositions were quantitatively analyzed by an electron probe microanalyzer (EPMA) in the same of the GeS_2 glass. The difference in composition between the first batch content and the prepared glasses were within 1 %.

2.2. Photoluminescence measurements

The setup for PL measurements has also been described in the previous report [33]. The time-dependent PL measurements were performed at 20 K-intervals from 10 K to 90 K for the main peak at 2.20 eV through prolonged irradiation by excitation light. It has additionally been measured at 110 K, 150 K for PL spectra, but the time dependence measurement was not performed. An argon-ion laser light with 457.9 nm of wavelength (2.71 eV) was used for excitation. The excitation intensity was 12 mW (0.7 W/cm^2). To obtain the evidence for the existence of another side-band at the foot of the main peak at lower temperatures, a He-Cd laser light with 441.6 nm of wavelength (2.81 eV), and 0.7 W/cm^2 of excitation intensity was used.

3. Results

Figs. 1 and 2 show the PL spectra for $Ge_{20}S_{80}$ and $Ge_{10}S_{90}$. Those for GeS_2 glass ($Ge_{33.3}S_{66.7}$) are given in Ref. 25. The PL intensity has a maximum at 30 K for GeS_2 glass, at below 10 K (~ 6 K) for $Ge_{20}S_{80}$, and at 10-50 K (~ 30 K) for $Ge_{10}S_{90}$. The compositional dependence of spectral shape of PL at 10 K is shown in Fig. 3. The spectra have a peak at

around 2.20 eV and are asymmetric shape especially for S-rich compositions.

The time-dependent peak intensities of the PL for $Ge_{20}S_{80}$ and $Ge_{10}S_{90}$ at 2.20 eV, measured at 10, 30, 50, 70 and 90 K are presented in Figs. 4 and 5. It is clearly observed that these behaviors strongly depend both on composition and temperature. The fitting functions were given and explained in Ref. 33. The time-dependent peak intensity of PL for GeS_2 was also presented. For $Ge_{20}S_{80}$ and $Ge_{10}S_{90,}$ different behaviors were observed at 10 K, and also at 30 K for $Ge_{20}S_{80}$.

The temperature dependence of the fatigue and recovery time constants, τ_F and $\tau_{R,}$ are presented in Figs. 6. and 7, which were estimated by fitting to the results in Figs. 4 and 5. The coefficients of fatigue and recovery, *A* and *B*, which were amplitude for the fatigue and recovery processes and described in detail in the previous chapter, are plotted in Figs. 8 and 9.

4. Discussion

4.1. Composition dependence of the photo-induced phenomena and side-band effects

An original model for the photoluminescence fatigue-recovery phenomena in Ge-S glass is described by Seki and Hachiya [29]. As discussed in Ref. 33, the full description of PL fatigue–recovery phenomena for GeS_2 glass for wide temperature range needs an extension of the function, which include side-band effect at cryogenic temperatures. Figs. 4 and 5 show the temperature dependence of the phenomena, although a large difference among compositions is observed. It is more clearly observed by He-Cd laser excitation (441.6 nm) the existence of another band at PL around 548 nm (2.26 eV) - 543 nm (2.28 eV). The PL spectra of side-bands by He-Cd laser excitation for $Ge_{33.3}S_{66.7}$, $Ge_{20}S_{80}$ and $Ge_{10}S_{90}$ at 10K are shown in Fig. 10. It is assumed from the spectra that the side-band has at least two different peaks.

The time-dependence at 10 and 70 K for Ar^+-ion laser excitation (457.9 nm),

compared with He-Cd laser excitation (441.6 nm), are presented in Figs. 11 (at 10 K) and 12 (at 70 K) for $Ge_{20}S_{80}$, and in Figs. 13 (at 10 K) and 14 (at 90 K) for $Ge_{10}S_{90}$. The side-band at 2.28 eV for $Ge_{33.3}S_{66.7}$ by Ar^{+}-ion laser excitation forms a high-energy tail of the main peak at 2.20 eV, as demonstrated in the previous study [33].

For Figs. 11 and 12 for $Ge_{20}S_{80}$, it is confirmed that the spectra has another peak at 2.25 eV, and the peak intensity change under prolonged irradiation, other than main peak at 2.20 eV. The side-band PL is included in total time dependence differently than that of main peak it measure at 2.20 eV, judging from the fatigue-recovery behaviors below 30 K for $Ge_{20}S_{80}$, and $Ge_{10}S_{90}$ along with $Ge_{33.3}S_{66.7}$ below 10 K. The side-band time-dependence become negligible compared with main peak for $Ge_{20}S_{80}$ over 70 K. Those of main peak and side-band peak are complementary, which are monotonic increasing and monotonic decreasing. These data can be fitted using the same function as Eq. (4) in Ref. 33 below 30 K as those of $Ge_{33.3}S_{66.7}$ below 10 K, but the time constants of third and fourth terms in the function, which describe side-band terms, are different.

On the other hand, the behavior of $Ge_{10}S_{90}$ in Figs. 13 and 14 are basically different from $Ge_{33.3}S_{66.7}$ and $Ge_{20}S_{80}$. The side-band PL of $Ge_{10}S_{90}$ at 2.28 eV does not change for prolonged irradiation, but the fatigue process for the main peak is clearly observed for each temperature in Figs. 5, 13 and 14. The different behavior of $Ge_{10}S_{90}$ originates from a time-dependent background intensity observed in the inset of Figs. 13 and 14, where the baseline of the spectra abruptly decreases. As already discussed for GeS_2 [33], only the side-bands at the high-energy-side of the main band were excited by He-Cd laser.

Fig. 15(a) and (b) show PL spectra excited by light of 457.9 nm, normalized by main peak and measured at 10 K and 70 K. A large decrease of background and those of side bands indicated by solid and broken arrows are observed. The side band spectra for the He-Cd excitation also exhibited a fatigue-recovery phenomenon for $Ge_{33.3}S_{66.7}$ and $Ge_{20}S_{80}$, while it was not observed other than the decrease of background for $Ge_{10}S_{90}$. The side bands

were not clearly observed in the spectra for Ar^+-ion laser (457.9 nm) excitation. For $Ge_{10}S_{90}$, the recovery process was not clearly observed within the present timescale even for 90 K.

The time-dependence of the PL intensity for this composition is then characterized by (i) fatigue process of main band, (ii) fatigue process of the extended background, and (iii) fatigue-recovery process of the side band at 2.25 eV (551 nm) to affect the peak-position intensity of main band at 2.20 eV.

$$I_{\mathrm{PL}}(t) = A\exp\left(-\frac{t}{\tau_{\mathrm{F}}}\right) + A^{E}\exp\left(-\frac{t}{\tau_{F}^{E}}\right) + A'\exp\left(-\frac{t}{\tau_{\mathrm{F551}}}\right) - B'\exp\left(-\frac{t}{\tau_{\mathrm{R551}}}\right) + I_{\infty} \qquad (1)$$

where the first term describes the fatigue process including the fatigue coefficient A and the fatigue time constant τ_{F}, and the second term described extend background instead of recovery terms, which was obscured below 90 K. The third and the fourth term are those affected by the side-band at 2.25 eV, whose band-shape is not clear compared with the band at 2.28 eV even by He-Cd laser excitation, although it is assumed as we have already done for GeS_2 and $Ge_{20}S_{80}$. It is rather observable as a side-band in Ar^+-ion-laser excitation spectra as shown in the inset figure of Fig. 13. The following simplified form is used for those above 30 K.

$$I_{\mathrm{PL}}(t) = A\exp\left(-\frac{t}{\tau_{\mathrm{F}}}\right) + A^{E}\exp\left(-\frac{t}{\tau_{F}^{E}}\right) + I_{\infty} \qquad (2)$$

The functional form with two fatigue terms successfully fit the experimental time-dependent PL intensities. A variety of behavior of time-dependent PL in Ge-S glass is summarized in Table1.

4.2. Composition dependence of the fatigue-recovery of photoluminescence phenomena in Ge-S glass

The fatigue-recovery phenomena in Ge-S system was described by using Eq. (4) in Ref. 33, which explicitly took the side-band effect below 10 K into consideration for

$Ge_{33.3}S_{66.7}$, and below 30 K for $Ge_{20}S_{80}$. As discussed above, Eqs. (1) and (2) were used instead for $Ge_{10}S_{90}$, where the recovery phenomena were not evident. As the time constant τ_R increased against decreasing temperature for all compositions, it is more dramatically increased up to 30,000 s for $Ge_{20}S_{80}$. On the other hand, τ_F does not change compare with τ_R and it was around 5,000-10,000 s. As discussed by Seki and Hachiya [29], τ_F is a function of power density of the photo-excited region, a function of laser power, while τ_R is the relaxation time of the temperature decrease, which is characteristic time for the thermal conduction in glass medium induced by temperature difference results from temperature increase through laser irradiation. It is reasonable that only τ_R depends on medium temperature.

Activation energy E_a, which determines the rate of fatigue and recovery process, can be estimated from the fit to Eq.(2) of Ref. 33 as demonstrated in Figs. 8 and 9, and in Fig. 4 of Ref. 33. It is around 10 meV estimated from both processes for $Ge_{33.3}S_{66.7}$ glass, 20 meV for $Ge_{20}S_{80}$ and 14 meV for fatigue process of $Ge_{10}S_{90}$. As shown in Fig. 3 of Seki et al. [28], relative stability of radiative centers against non-radiative centers depends strongly on sulfur content, which results in strong dependence of radiative center population on sulfur content, and in difference of ESR-signal and PL intensities [28-30]. Increase of E_a from x = 66.7 to 80 ($Ge_{1-x}S_x$) and decrease from x = 80 to 90 correspond to increase and decrease of activation energy, respectively, which is needed to suppress and proceed the recovery reaction in this case, the reaction from non-radiative to radiative centers. Increase of E_a causes degradation of PL intensity which is observed between x = 66.7 to 80, and promotion of PL intensity between x = 80 to 90 [28] as a result of the decrease/increase of radiative center population through suppression/promotion of the recovery reaction. All of these experimental results are mutually consistent only when we take the recovery process into consideration. The transient PL intensity measurement reaches to steady state finally after recovery process which follows fatigue process. This fact also means that the recovery

process is the rate-limiting process.

The above values are reasonably small to be achieved in the present photo-induced process assisted by heat and light. For all compositions, both BT^2 and AT^2 shifted upward from Arrhenius-type behavior at lower temperatures. The results indicate that the rate of the recovery process and that of the fatigue process relatively increases at lower temperatures. As we will discuss below, this discussion is confirmed within ground and first excitation states of the main-band photoluminescence process.

Presented in Fig. 16 is a possible model for the excitation-radiation mechanism in this study, not only main PL band (2.22 eV) but sub-bands (2.25 and 2.28 eV) being taken into account. These sub-bands were revealed in this study partly because we used shorter wavelength of light with He-Cd laser additionally, and because PL spectra were measured at lower temperatures compared with previous studies [28-30]. In such case, we can assume second excited states for both charged and neutral pair of defects to be located slightly above those for the first excited states with higher excitation energy, the following features would be enough to explain results summarized in Table 1: (i) radiative centers for main PL at 2.22 eV have second excitation states a** above first states a* and energy barriers (e2-c2 and e2-h2) between a** (c2) and second states h2; (ii) the second excitation states h2 above first states f* for non-radiative recombination (f-g-f*-f) for neutral defects [29] are radiative this time. If the sub-band at 2.25 eV is for radiation from second excited states for neutral defects (h2-i), the time-dependence which is contrary to main-band fatigure-recovery can be explained. On the other hand, if the sub-band at 2.28 eV is for c2-d, the difference from sub-band in 2.25 eV in time-dependence is possible, which is observed as presented in Table 1. The difference in height of energy barriers (activation energy) from both sides (difference in e2-c2 and e2-h2) depends on sulfur content, and that will account for presence and absence of 2.25 or 2.28 eV sub-bands in Table 1. Furthermore, as can be seen in Fig. 16, the reversal of relative advantage of fatigue reaction over recovery in the second

excited states from that of the first excited states for the main-band PL also results in higher activation energy required to c2 to h2 reaction, and therefore, the absence of time-dependence in side-band 2 as a consequence. The composition dependence may also explain relatively strong sub-bands above, other bands at 2.35, 2.40, … eV and backgrounds for $Ge_{10}S_{90}$ glass even for Ar^+-laser excitation, if the second excited states and possibly the higher states are slightly lower for this glass composition. The dependence is naturally reflected in configuration of ground states and first excitation states, which results in variation of fatigue/recovery time constants of main PL band.

5. Conclusions

The time-dependent photoluminescence and its temperature-dependence for several compositions ($Ge_{33.3}S_{66.7}$, $Ge_{20}S_{80}$ and $Ge_{10}S_{90}$) were investigated.

Side-band effects were considered to fully describe the time dependence, one band at 2.25 eV for all compositions and the other extended from 2.15 to 2.45 for $Ge_{10}S_{90}$, especially at the lower temperatures.

Another side-band at 2.28 eV, which is apparently time-independent, was also analyzed.

The functional form was similar to those in the previous report, and was extended to account for the effect of side-band at below 30 K for $Ge_{20}S_{80}$ and monotonous decrease of background for $Ge_{10}S_{90}$.

Acknowledgments

We thank T. Goto, T. Nohira, R. Hagiwara, K. Ema, H. Shiino and M. Seki for their supports and helpful discussions. A part of this work is supported by a Grant-in-Aid for Scientific Research (C) (23561030) from the Japan Society for the Promotion of Science (JSPS).

References

[1] A. V. Kolobov, P. Fons, A. I. Frenkel, A. L. Ankudinov, J. Tominaga, T. Uraga, *Nature Materials* **3** (2004) 703.

[2] T. Kawaguchi, S. Maruno, *Jpn. J. Appl. Phys.* **27** (1988) 2199.

[3] L. Qimingn, G. Fuxi, *Materials Lett.* **53** (2002) 411.

[4] T. Tada and T. Ninomiya, *J. Non-Cryst. Solids* **137-138** (1991) 997.

[5] K. Shimakawa, S. Inari, T. Kato, S. R. Elliot, *Phys. Rev.* B **46** (1992) 10062.

[6] S.H. Massaddeq, M. Siu Li, D. Lezal, S. J. L. Ribeiro, Y. Messaddeq, *J. Non-Cryst. Solids* **284** (2001) 282.

[7] S. R. Elliot, *Physics of Amorphous Materials, 2nd. Edition*, (Longman, London, 1990).

[8] F. Mollot, J. Cernogora, and C.Benoit à la Guillaume, *Phil. Mag. B* **42** (1980) 643.

[9] K. Shimakawa , A. Kolobov and S. R. Elliot, *Adv. Phys.* **44** (1995) 475.

[10] T. Tada and T. Ninomiya, *J. Non-Cryst. Solids* **137-138** (1991) 997.

[11] M. J. Chamberlain and J. A. Moseley, *J. Phys. C: Solid State Phys.* **16** (1983) 1987.

[12] R. A. Street and N. F. Mott, *Phys. Rev. Lett.* **35** (1975) 1293.

[13] M. Kanstner, D. Adler and H. Fritzsche, *Phys. Rev. Lett.* **37** (1976) 1504.

[14] M. H. Cohen, H. Fritzsche and S. R. Ovshinsky, *Phys. Rev. Lett.* **22** (1969) 1065.

[15] E. A. Davis and N. F. Mott, *Phil. Mag.* **22**, (1970) 903.

[16] N. F. Mott, E. A. Davis and R. A. Street, *Phil. Mag.* **32** (1975) 961.

[17] M. Kastner and H. Fritzsche, *Phil. Mag.* B**37** (1978) 199.

[18] M. Popescu, *Photo-Induced Metastability in Amorphous Semiconductors,* Ed. by A.V. Kolobov. (Wileky-VCH, Weinheim, 2003), Chapter 1.

[19] Y. Kuzukawa, A. Ganjoo, and K. Shimakawa, *Phil. Mag.* B**79** (1999) 249.

[20] A.V. Kolobov (Ed), *Photo-Induced Metastability in Amorphous Semiconductors,* (Wileky-VCH, Weinheim, 2003), Chapter 18-23.

[21] K. Arai, U. Itoh, H. Namikawa, *Jpn. J. Appl. Phys.* **13** (1974) 1305.

[22] Y. Wada, Y. Wang, O. Matsuda, K. Inoue, K. Murase, *J. Non-Cryst. Solids* **198–200** (1996) 732.

[23] V.K. Tikhomirov, K. Iakoubovskii, P.W. Hertogen, G.J. Adriaenssens, *Appl. Phys. Lett.* **71** (1997) 2740.

[24] N.V. Bondar, N.A. Davydova, V.V. Tishchenko, M. Vlcek, *J. Molec. Struct.* **555** (2000) 175.

[25] E. Černošková, Z. Černošek, A. Henry, K. Swiatek, M. Frumar, *Mater. Lett.* **25** (1995) 21.

[26] K. Tanaka, Y. Kasanuki, A. Odajima, *Thin Solid Films* **117** (1984) 251.

[27] Y. Watanabe, H. Kawazoe, M. Yamane, *Phys. Rev.* B **38** (1988) 5668.

[28] M. Seki, K. Hachiya, K. Yoshida, *J. Non-Cryst. Solids* **315** (2003) 107.

[29] M. Seki, K. Hachiya, *J. Phys.: Condens. Matter* **15** (2003) 4555.

[30] M. Seki, K. Hachiya, K.Yoshida, *J. Non-Cryst. Solids* **324** (2003) 127.

[31] K. Hachiya, *J. Non-Cryst. Solids* **312-314** (2002) 566.

[32] K. Hachiya, *J. Non-Cryst. Solids* **321** (2003) 217.

[33] T. Nakanishi, Y. Tomii, K. Hachiya, *J. Non-Cryst. Solids* **354** (2008) 1627.

[34] H. Takebe, H. Maeda, K. Morinaga, *J. Non-Cryst. Solids* **291** (2001) 14-24.

[35] G. Saffarini, Appl. Phys. A. **59** (1994) 385.

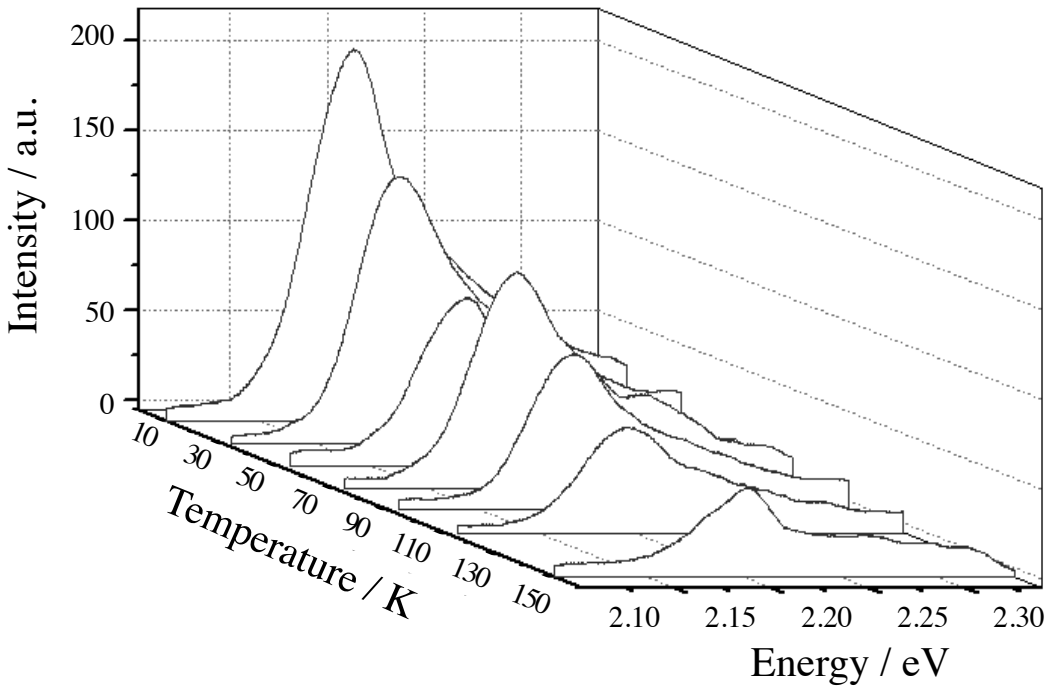

Fig. 1 The PL spectra for $Ge_{20}S_{80}$ at 10, 30, 50, 70, 90, 110 and 150 K.

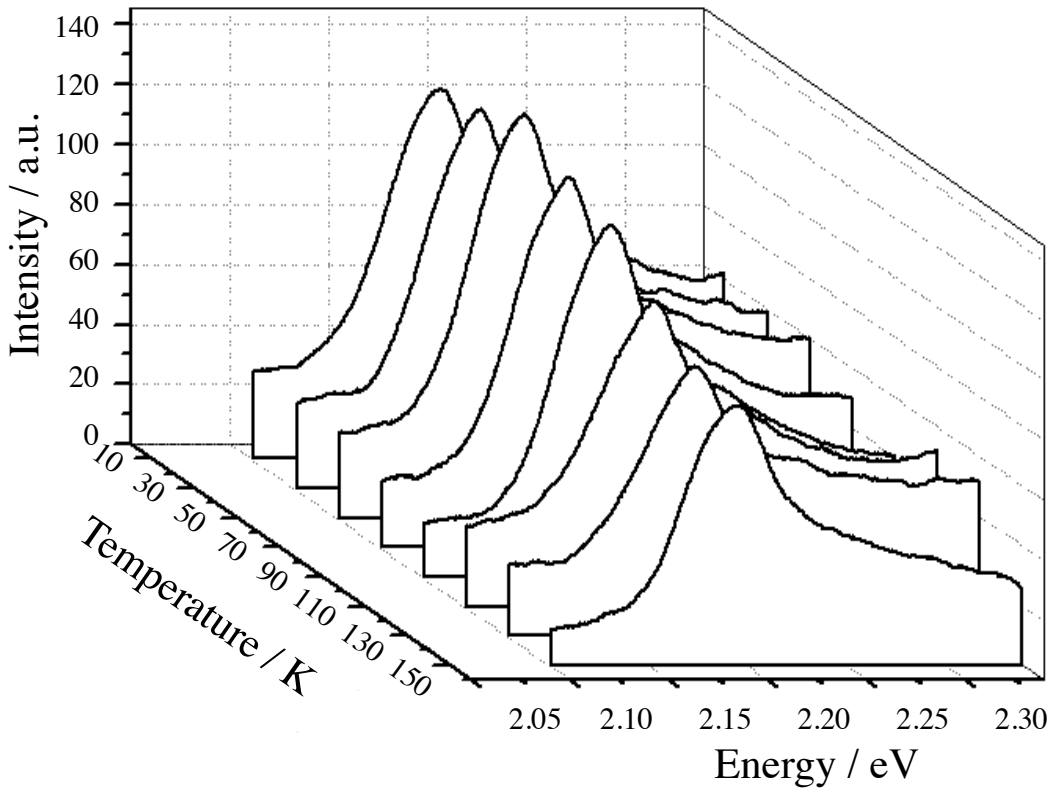

Fig. 2 The PL spectra for $Ge_{10}S_{90}$ at 10, 30, 50, 70, 90, 110, 130 and 150 K.

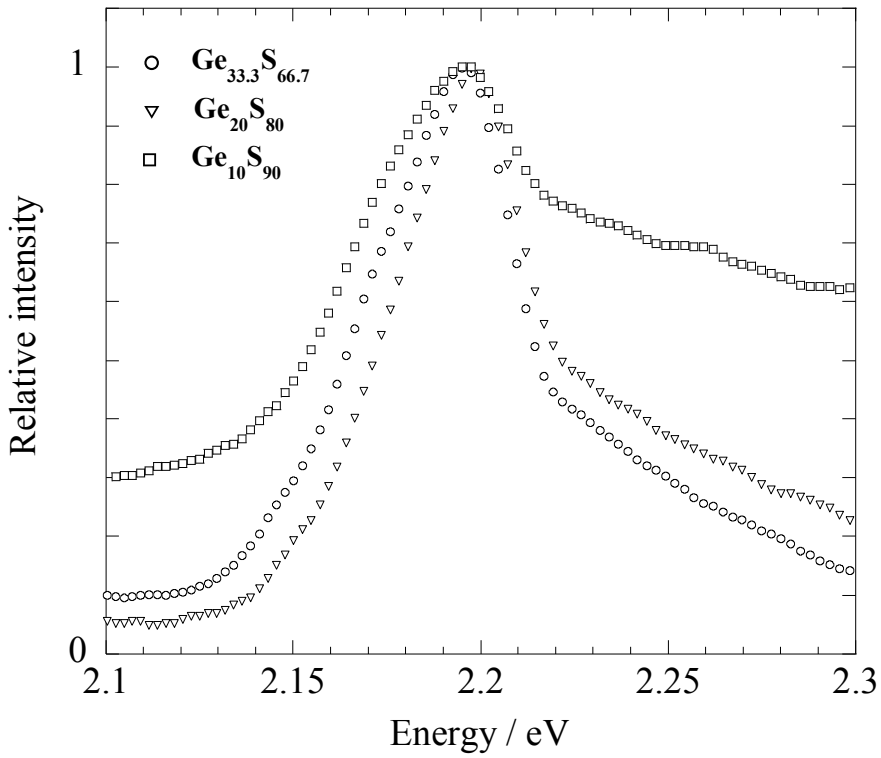

Fig. 3 The PL spectra of $Ge_{33.3}S_{66.7}$ (GeS_2), $Ge_{20}S_{80}$ and $Ge_{10}S_{90}$ at 10 K and normalized at peak position.

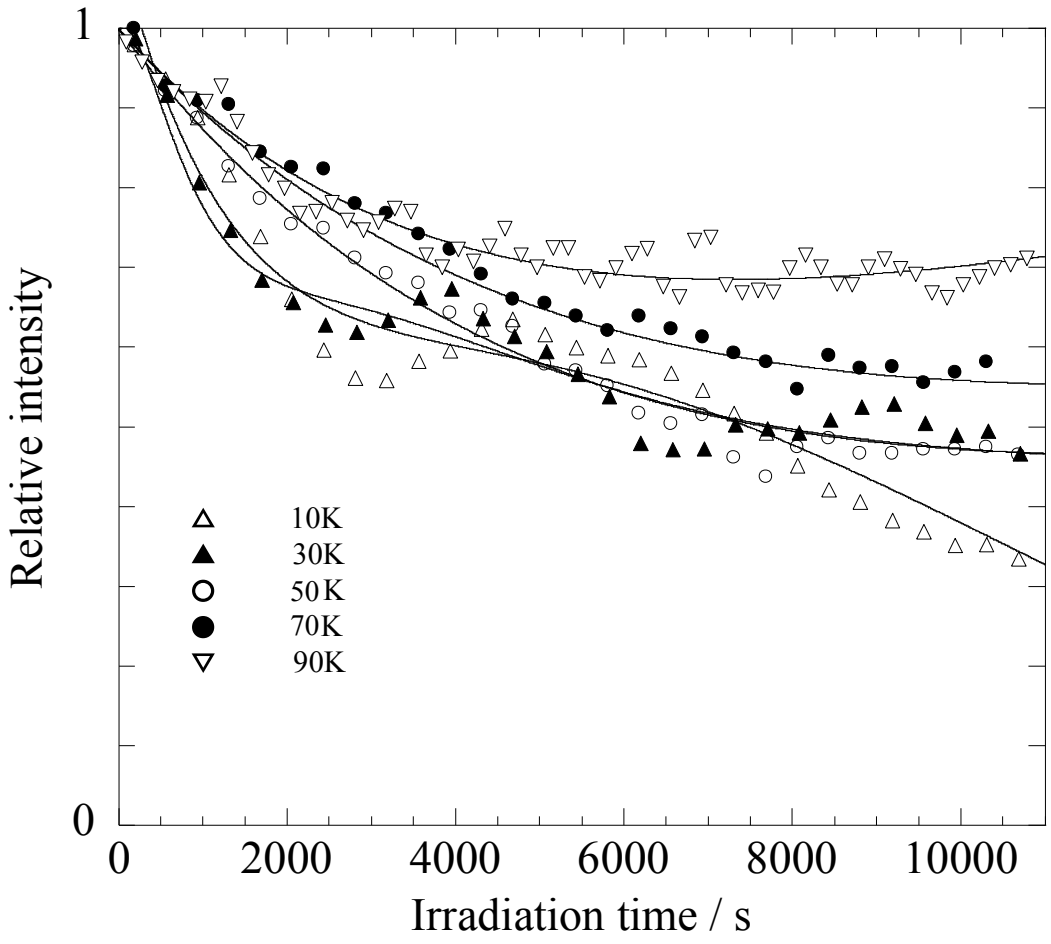

Fig. 4 The time dependence of the PL at 2.20 eV in $Ge_{20}S_{80}$ glass at 10, 30, 50, 70 and 90 K. The full curves are the fits using Eq. (4) in Ref. 25 for 10 and 30 K, and Eq. (1) in Ref. 25 for other temperatures.

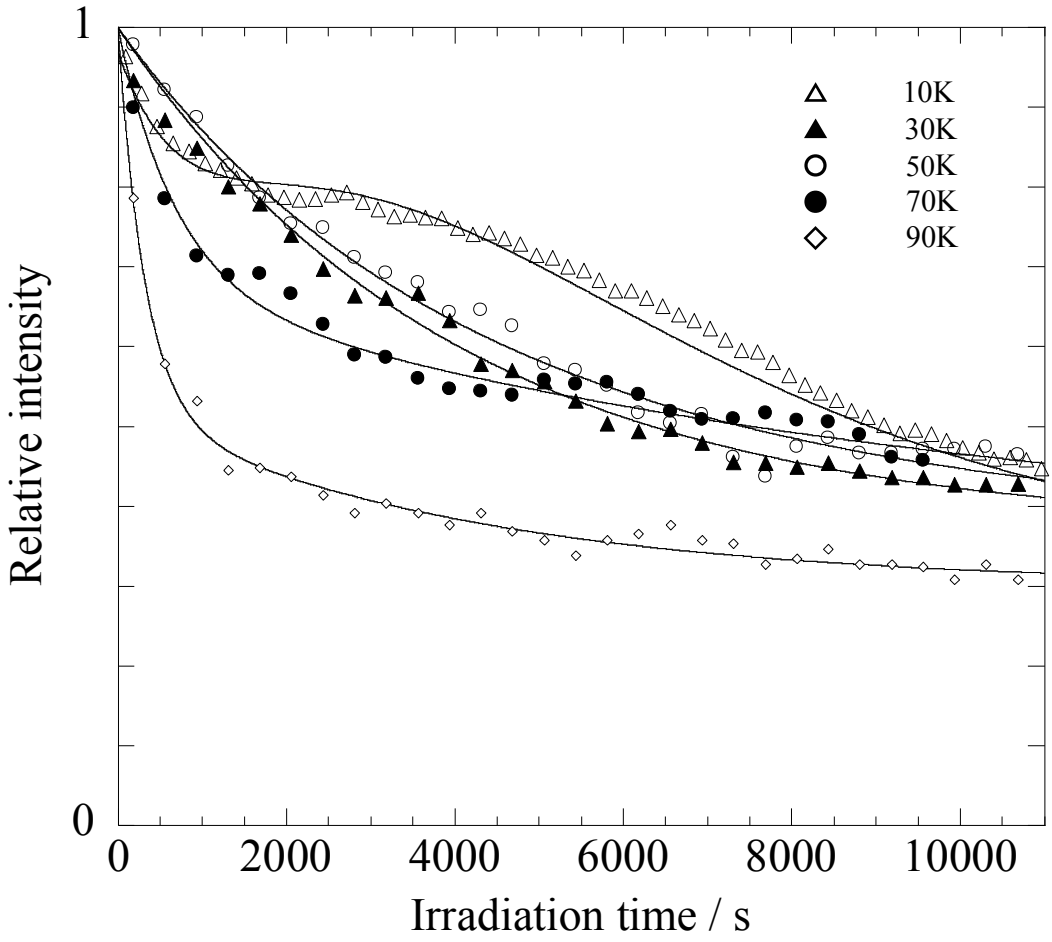

Fig. 5 The time dependence of the PL at 2.20 eV in $Ge_{10}S_{90}$ glass at various temperatures. The full curves are the fits using Eq. (1) for 10 K, and Eq. (2) for other temperatures.

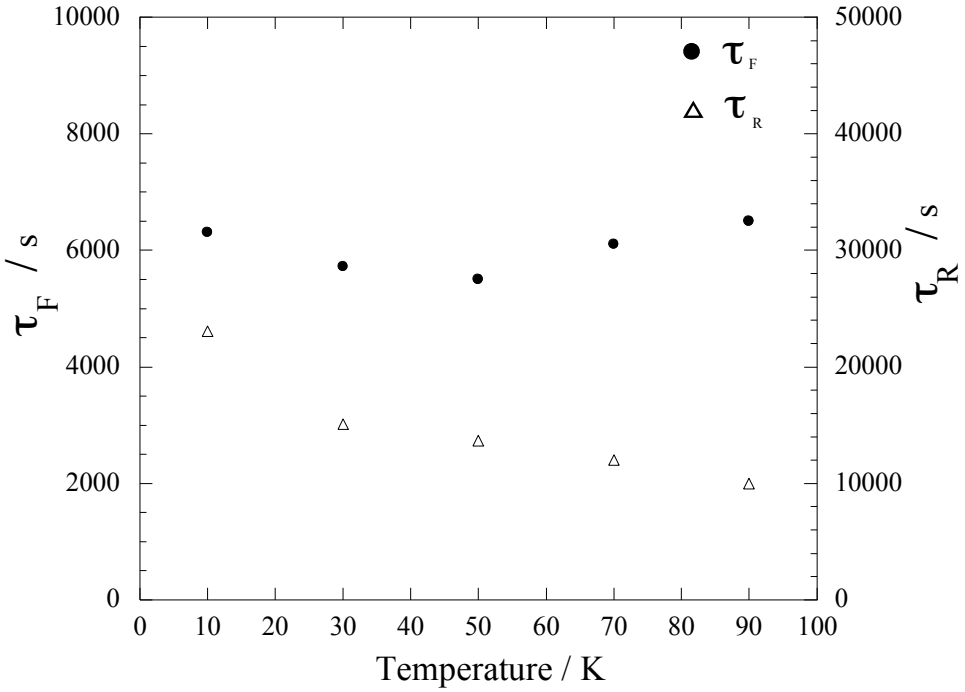

Fig. 6 The time constants τ_F, τ_R, are plotted from using the results by fitting for Fig. 4 at cryogenic temperatures.

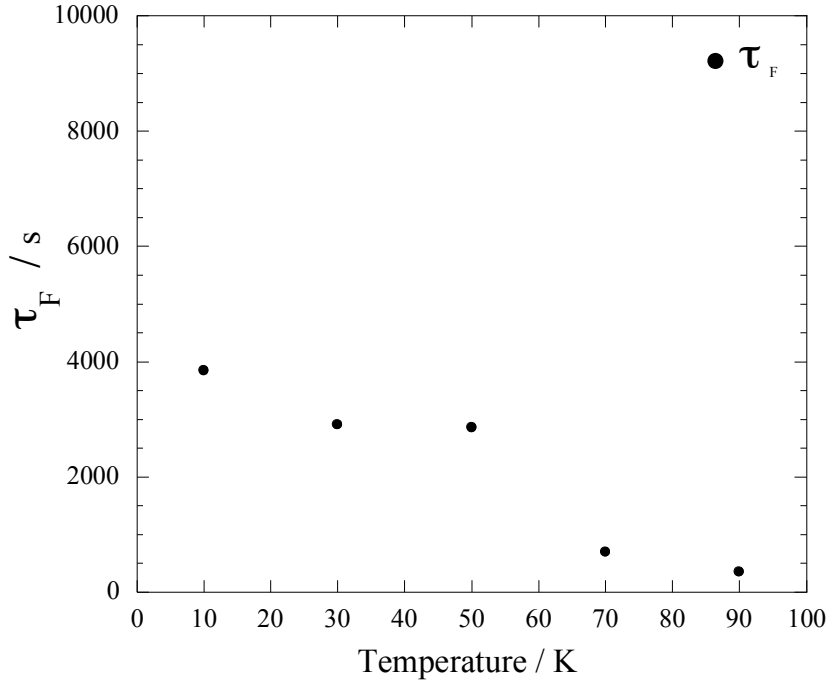

Fig. 7 The time constants, τ_R, is plotted from using the results by fitting for Fig. 5 at cryogenic temperatures.

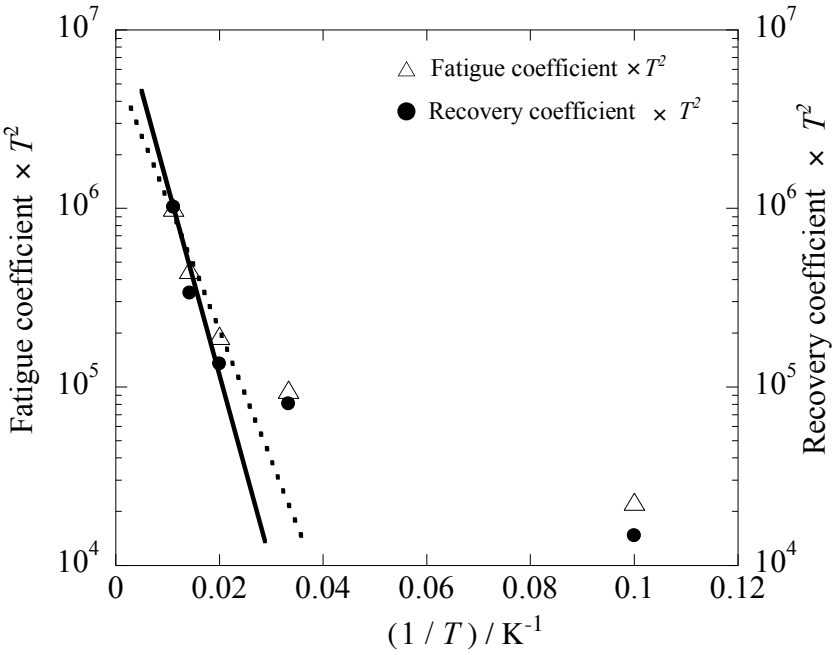

Fig. 8 The coefficients for fatigue and recovery multiplied by T^2, AT^2 and BT^2, estimated by fitting of A and B. Solid line and broken line are drawn for guides for the eye.

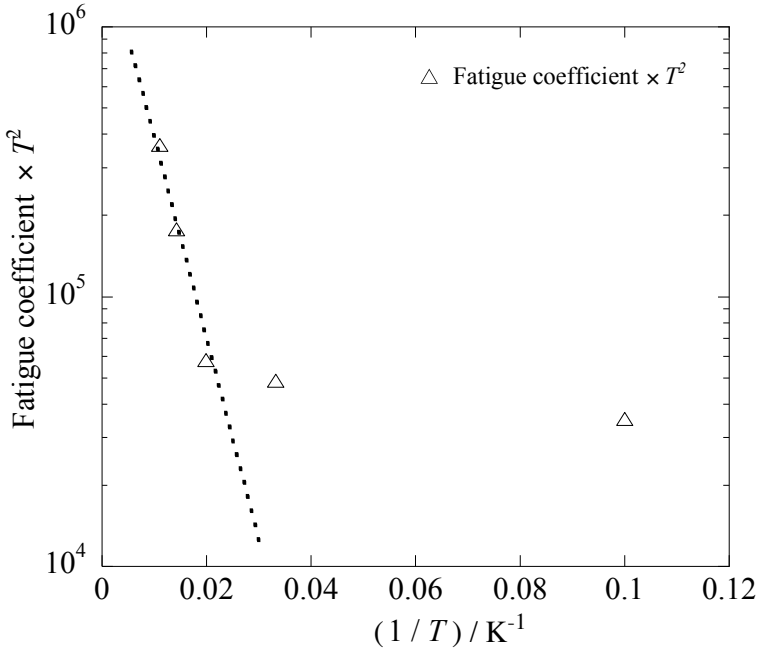

Fig. 9 The coefficients for fatigue and recovery multiplied by T^2, AT^2, estimated by fitting of A. Broken line are drawn as a guide for the eye.

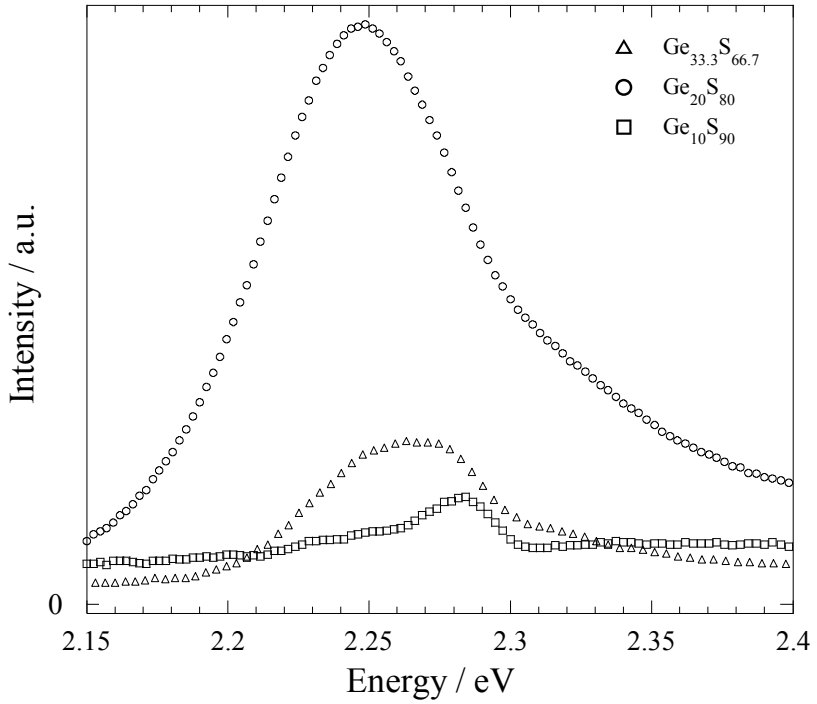

Fig. 10 The PL spectra for $Ge_{33.3}S_{66.7}$, $Ge_{20}S_{80}$ and $Ge_{10}S_{90}$ glasses observed at 10 K. The excitation energy is 441.6 nm (2.81 eV) and intensity is 12 mW with He-Cd laser.

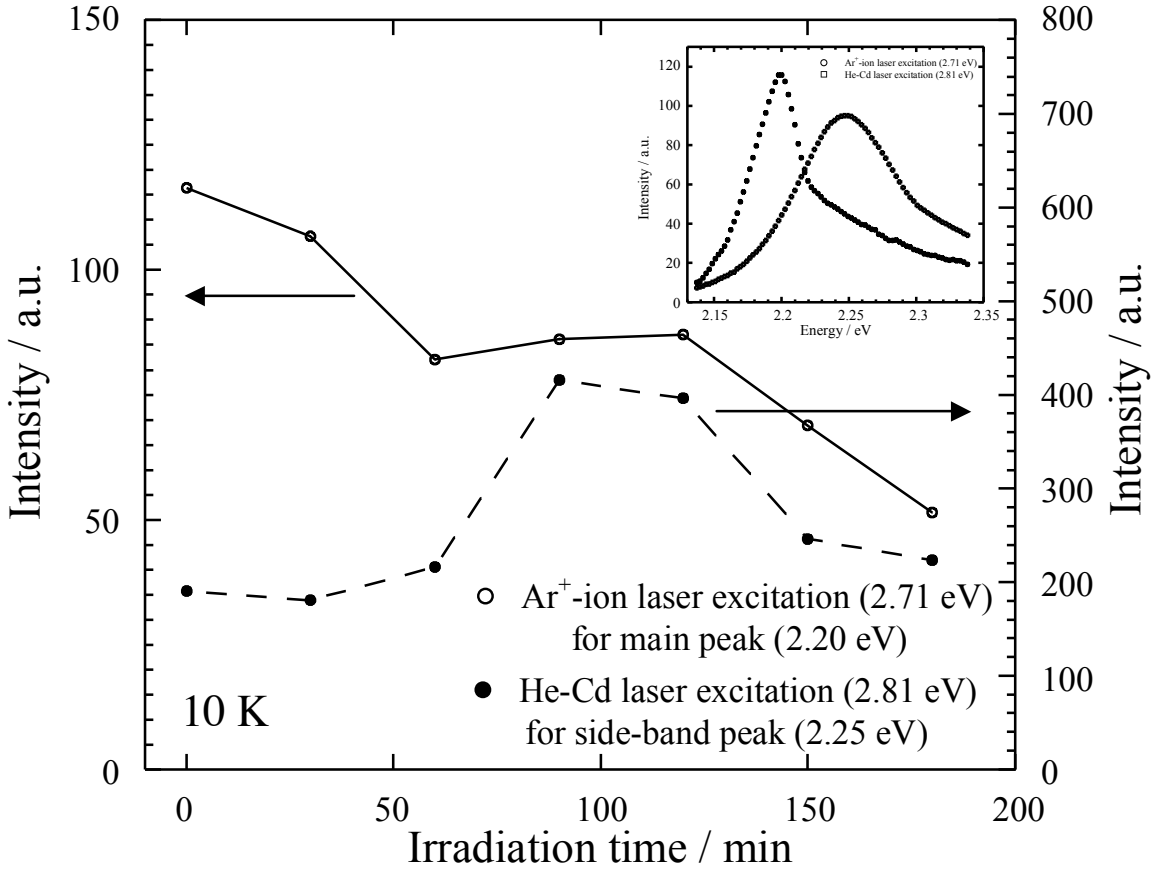

Fig. 11 The time dependence of the PL intensity for main band (2.20 eV) and side-band (2.25 eV) for $Ge_{20}S_{80}$ at 10 K. The inset is the PL spectra excited by Ar^+-ion laser of 457.9 nm(2.71 eV) and He-Cd laser with 441.6 nm (2.81 eV).

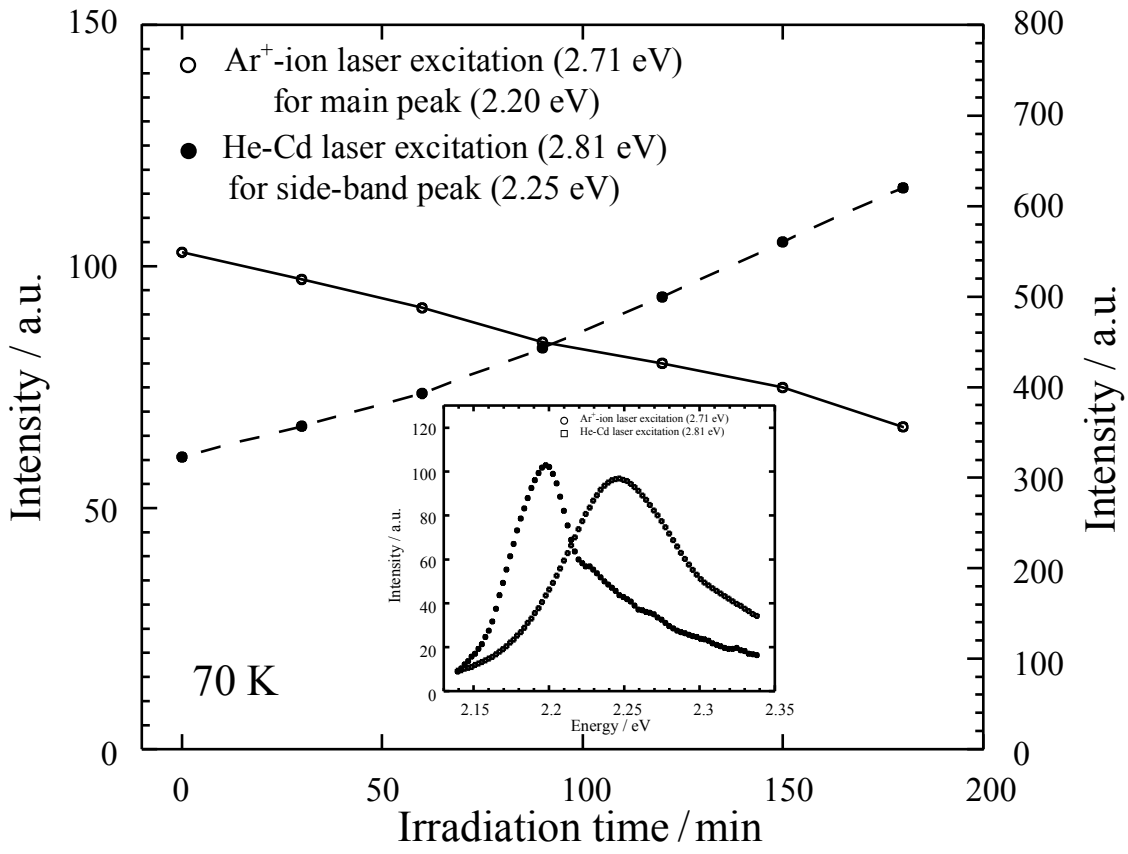

Fig. 12 The time dependence of the PL intensity for main band (2.20 eV) and side-band (2.25 eV) for $Ge_{20}S_{80}$ at 70 K. The inset is the PL spectra excited by Ar^{+}-ion laser of 457.9 nm (2.71 eV) and He-Cd laser with 441.6 nm (2.81 eV).

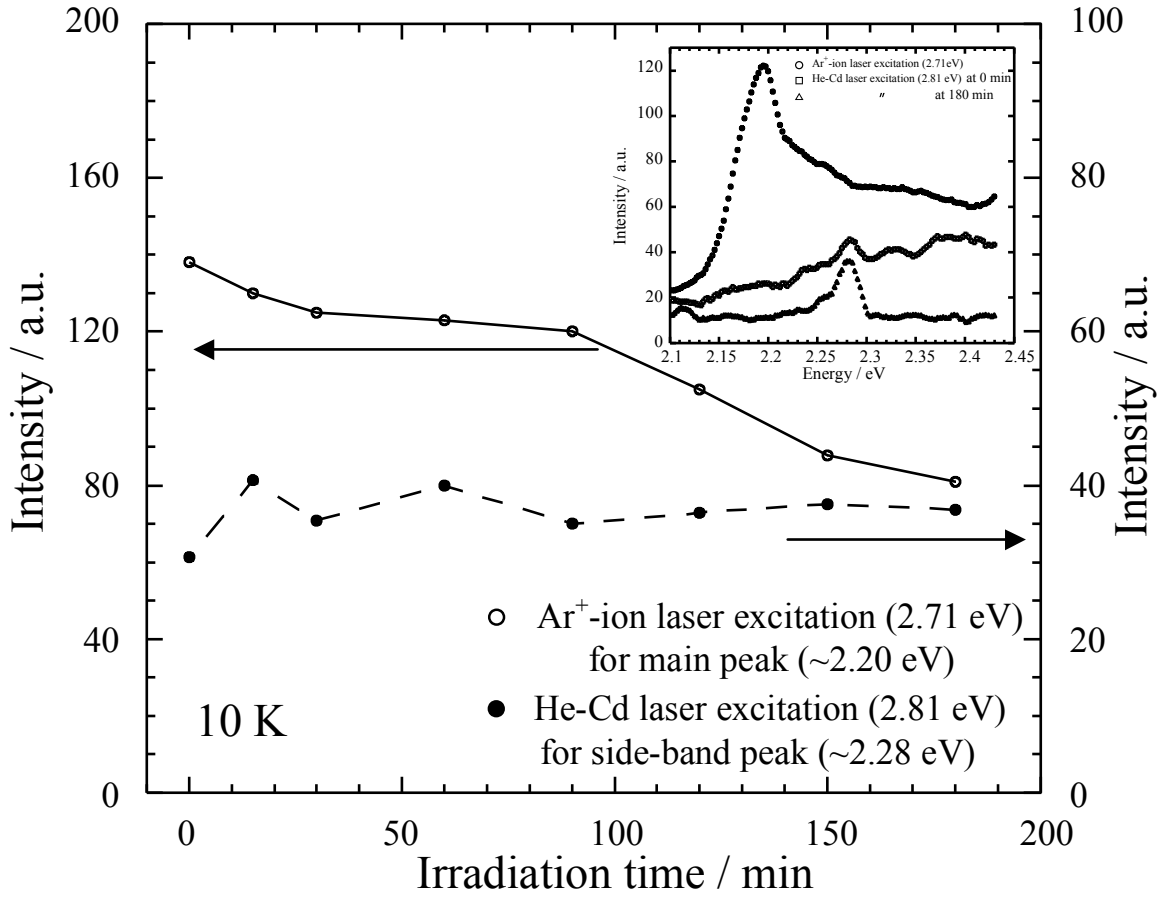

Fig. 13 The time dependence of the PL intensity for main band (2.20 eV) and side-band (2.28 eV) for $Ge_{10}S_{90}$ at 10 K. The inset is the PL spectra excited by Ar^+-ion laser of 457.9 nm (2.71 eV) and He-Cd laser with 441.6 nm (2.81 eV). The solid and broken lines are to additional lines.

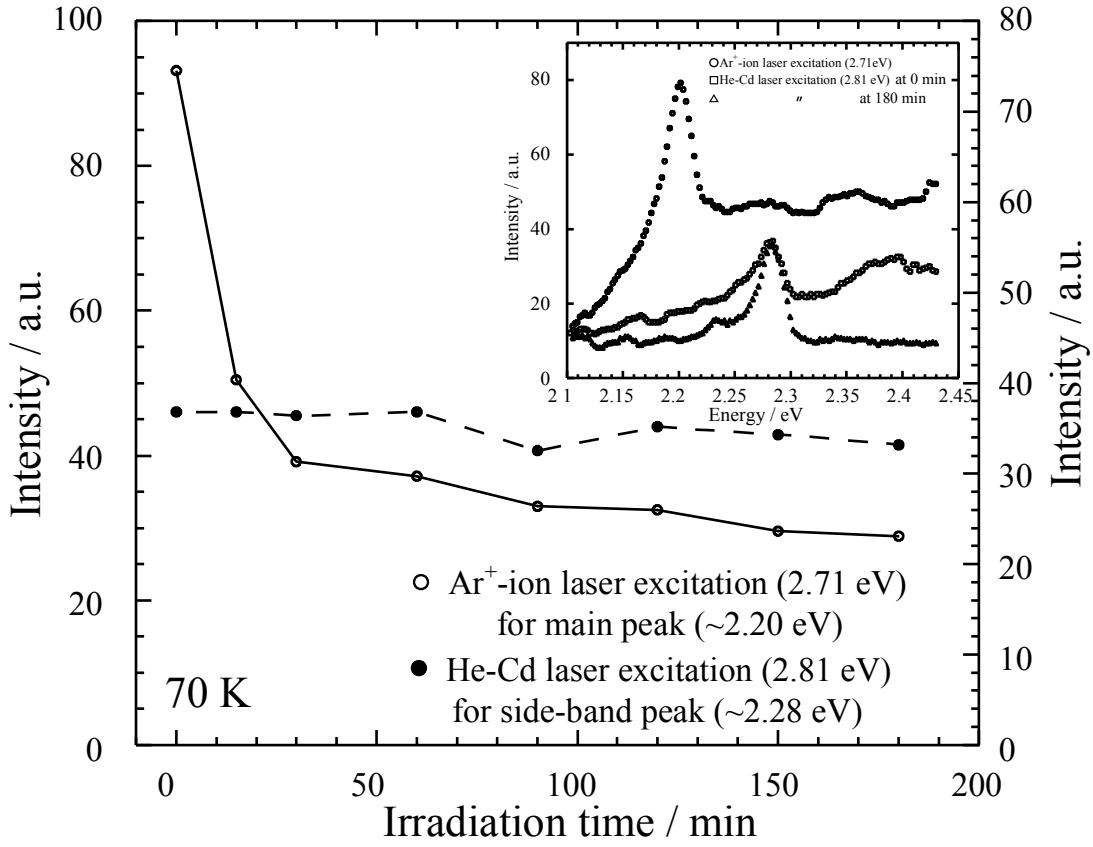

Fig. 14 The time dependence of the PL intensity for main band (2.20 eV) and side-band (2.28 eV) for $Ge_{10}S_{90}$ at 90 K. The inset is the PL spectra excited by Ar^+-ion laser of 457.9 nm (2.71 eV) and He-Cd laser with 441.6 nm (2.81 eV).

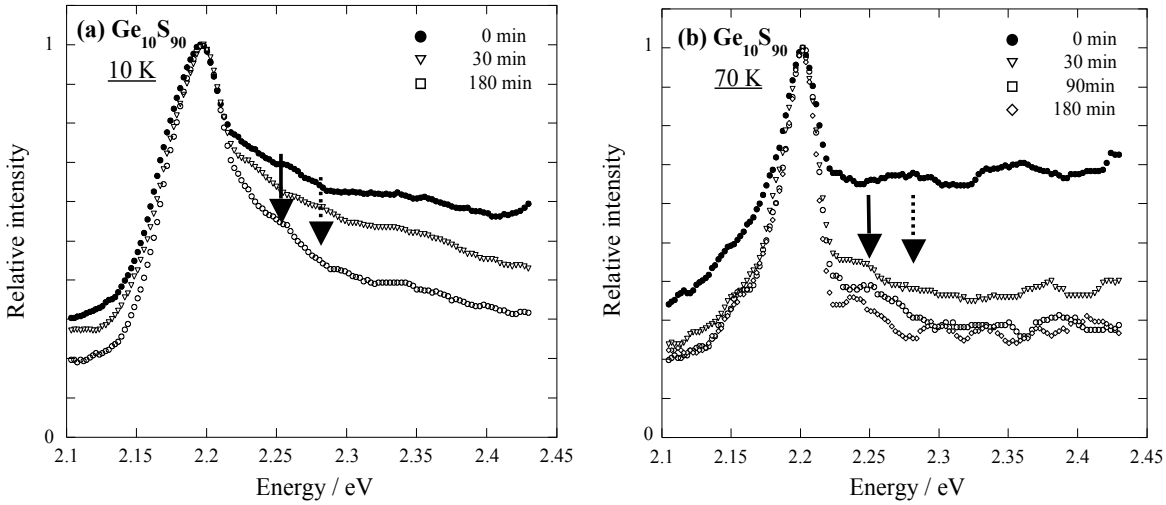

Fig. 15 The PL spectra of $Ge_{10}S_{90}$ glass measured the passage of time: 0, 30 and 180 min at 10 K (a) and: 0, 30, 90 and 180 min at 70 K (b) normalized at main-band peak position.

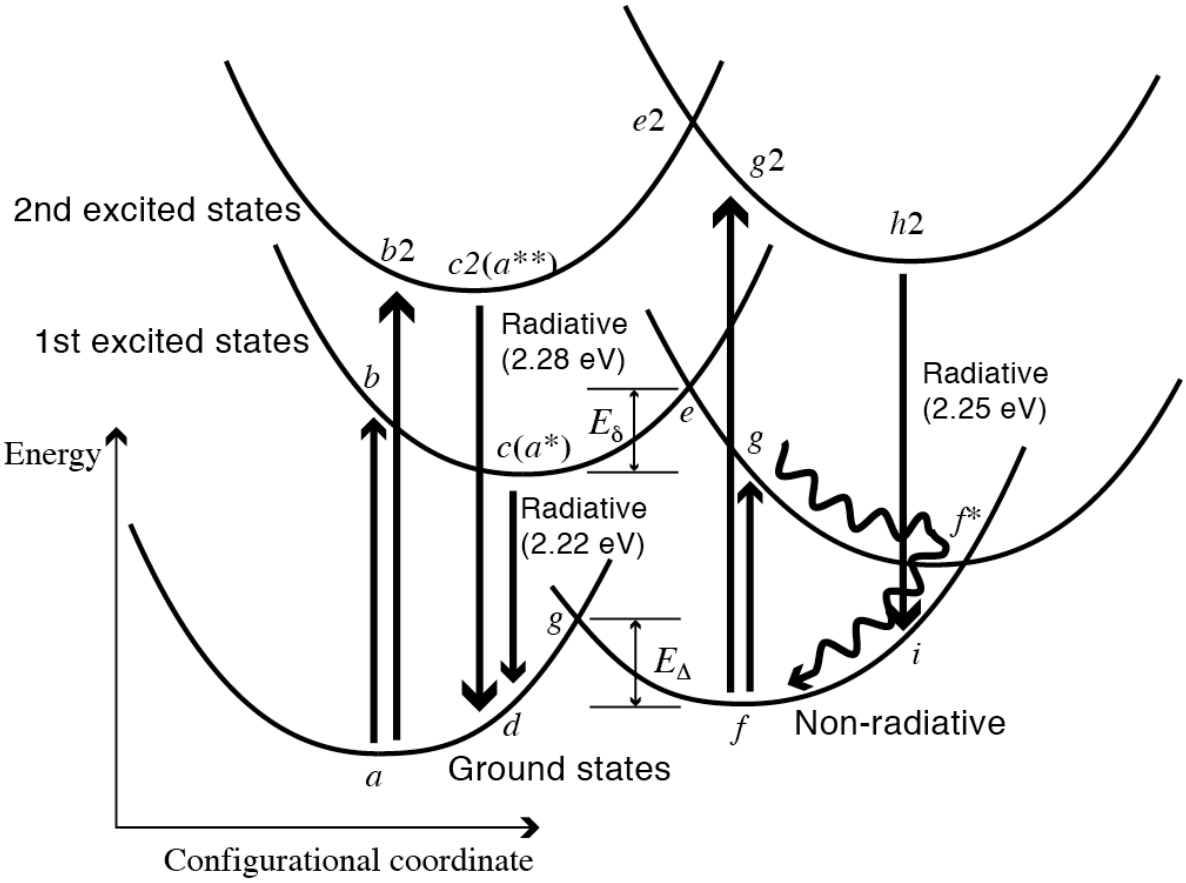

Fig. 16　A Schematic for the excitation-radiation process for the main-band and side-band photoluminescence emission mechanism.

Table.1 PL bands and their time-dependent phenomena in Ge-S glass.

PL bands	Time dependence	$Ge_{33.3}S_{66.7}$	$Ge_{20}S_{80}$	$Ge_{10}S_{90}$
		Ar^+-ion laser (2.71 eV) excitation		
Main peak 2.20 eV	F-R	Strong	Strong	Strong (F)
		He-Cd laser (2.81 eV) excitation		
Side-band 1 2.25 eV	R-F	Strong, below 10 K	Strong, below 30 K	Weak, below 10 K
Side-band 2 2.28 eV	–	Weak	–	Strong
Background 2.15-2.45 eV	F	–	–	Strong

F: Fatigue process; R: Recovery process